View metadata, citation and similar papers at core.ac.uk

brought to you by CORE

provided by NASA Technical Reports Server

NASA-CR-196331

IN-33-CR
OCIT
26421
33P

RAMAN STRUCTURAL STUDIES OF THE NICKEL ELECTRODE

(Power Systems Division)
(Grant NAG 3-519)

FINAL REPORT

Research Conducted:
Feb. 20, 1984 - Oct. 31, 1991

Report Submitted:
September 7, 1994

Bahne C. Cornilsen
Michigan Technological University
Department of Chemistry
1400 Townsend Dr.
Houghton, Michigan 49931-1295

Sponsor:

University Grants Office
National Aeronautics and Space Administration
Lewis Research Center
21000 Brookpark Avenue
Cleveland, Ohio 44135

N95-13344
Unclas
G3/33 0026421

(NASA-CR-196331) RAMAN STRUCTURAL STUDIES OF THE NICKEL ELECTRODE Final Report, 20 Feb. 1984 - 31 Oct. 1991 (Michigan Technological Univ.) 33 p

PRECEDING PAGE BLANK NOT FILMED

SUMMARY

The objectives of this investigation have been to define the structures of charged active mass, discharged active mass, and related precursor materials (α-phases), with the purpose of better understanding the chemical and electrochemical reactions, including failure mechanisms and cobalt incorporation, so that the nickel electrode may be improved. Although our primary tool has been Raman spectroscopy, the structural conclusions drawn from the Raman data have been supported and augmented by three other analysis methods: infrared spectroscopy, powder X-ray Diffraction (XRD), and x-ray absorption spectroscopy (in particular EXAFS, Extended X-ray Absorption Fine Structure, spectroscopy).

Raman spectroscopy provides unique structural information that is not clearly obtainable via other structural analysis methods (in particular diffraction), in that the Raman selection rules and Raman spectra differ for close packed vs non-close packed layered structures. This unique feature is demonstrated for the two best characterized materials, ordered β-$Ni(OH)_2$ and γ-NiOOH. The former displays close packed NiO_2 layers (ABAB stacking) and the latter, non-close packed NiO_2 layers (ABBCCA stacking). If two materials have similar selection rules (*i.e.* similar Raman spectra in terms of numbers and relative intensities of bands), then the structures may be judged to be the same. The four commonly defined phases of active mass (in the α/γ and β/β cycles) display similar selection rules. Therefore, we conclude that these four materials exhibit a common non-close packed structure (ABBCCA NiO_2 layer stacking). The phases known as γ-, γ_1-, and γ_2-NiOOH are shown to be $Ni_{1-x}V_xOOH_{1-y}$ or $Ni_{1-x}K_xOOH_{1-y}$, not $KNi_2O_3 \cdot nH_2O$. That discharged active mass does <u>not</u> display a close packed β-type structure is significant; it should not be referred to as β-$Ni(OH)_2$.

Although they display similar layer stacking, these four materials (in the α/γ and β/β cycles) do differ in terms of potassium and hydrogen content, nickel vacancy content, density, and nickel oxidation state. These differences are reflected in the precise Raman band positions observed, and in the empirical formulae observed for each material. Based on the unit cell symmetry and these empirical formulae, structural formulae have been proposed which show that the major structural differences can be simply understood on the basis of a nonstoichiometric point defect structural model.

Since β-$Ni(OH)_2$ is not the "active" material in active mass, the presence of β-$Ni(OH)_2$ may be detrimental to battery performance. (The reasons that discharged active mass came to be erroneously known as a β-type material are discussed and explained.) Indeed, the "deactivated" materials defined by Bernard *et al.* are shown to be disordered β-$Ni(OH)_2$ phases which are nonstoichiometric and contain point defects.

The Raman spectra of precursor α-phases (cathodically deposited and chemically deposited) show that they too differ in structure from β-$Ni(OH)_2$ and from discharged active mass. We propose a non-close packed structure for these α-phase materials. The Raman spectra

demonstrate that these precursors have a structure similar to discharged active mass (non-close packed), yet different; the need for the electrode "formation process" is understood in that it transforms the precursor structure into that which is more active (and therefore termed "active mass"). The beneficial roll of cobalt addition is seen in terms of a stabilization effect, stabilizing the more favorable active mass structure, during cycling.

The formation of detrimental second phases is an expected electrode failure mechanism. Although often proposed in the literature, the occurrence of such a second phase has not been previously documented. A "new phase" has been found using Raman spectroscopy; this phase forms in electrolyte of high KOH concentration, and its presence correlates with electrode failure.

The structural understanding that has been developed for actual "active mass" (containing cobalt) in this study has been made possible by the careful analysis and preparation of "model compounds," materials that have been carefully defined in the literature, found to be reproducibly prepared by us and others, and found to be single phase materials. The structural models for these materials are supported by all four instrumental analysis methods.

CONTENTS

INTRODUCTION

The goal of structural characterization of nickel electrode materials is to define the relationship between chemical structure and electrochemical properties; this understanding will allow development of improved electrodes. The objectives of this investigation have been to define the structures of charged active mass, discharged active mass, and related precursor materials, with the purpose of better understanding the chemical and electrochemical reactions, including failure mechanisms.

Polycrystalline nickel electrode materials are difficult to characterize structurally because of disorder and their fine particle size. Furthermore, formation on a nickel metal substrate or other conducting material complicates many instrumental analyses, often making *in situ* measurements difficult or impossible. Raman spectroscopy is an ideal technique for the study of such polycrystalline systems, including the ability to make aqueous, *in situ* measurements.

Structural differences have been observed using Raman spectroscopy which have been induced by charge/discharge, cobalt doping, electrode preparation conditions (deposition variables), ageing in KOH, and the formation process. Differences have been observed which escaped detection using other methods (1-6), in particular the ability to distinguish the difference between two different inter-layer NiO_2 stacking arrangements. (Intra-layer stacking, *i.e.* within an NiO_2 layer is close packed.)

Key structural conclusions about electrochemical active mass (β/β and α/γ cycles) have been based on this unique difference between the Raman spectra for layered materials with close packed vs non-close packed NiO_2 layer stacking (5,7,8). Chemically precipitated and oxidized NiOOH is non-close packed and β-$Ni(OH)_2$ phases are close packed. Raman spectra of active mass in both electrochemical cycles (β/β and α/γ) shows that all four phases are non-close packed. Chemically prepared phases (α- and β-nickel hydroxides) have traditionally been considered to be structural models for the electrochemical materials. Our results indicate that there are significant differences between the latter structures as reflected by the Raman spectra.

A variety of electrode types have been studied, including commercial electrodes, NASA samples, as well as plaque and nickel foil electrodes prepared ourselves. The influence of KOH concentration on cycle life and failure mechanism has been studied on electrodes obtained from a NASA supported study at Hughes Aircraft (9). A "new phase" has been identified using Raman spectroscopy (10,11). Several additional methods have been used to characterize the samples, including infrared spectroscopy, thermogravimetric analysis (TGA), cyclic voltammetry, and wet chemical analysis of nickel, dopants, and active oxygen.

EXPERIMENTAL: PREPARATIONS AND INSTRUMENTATION

Samples characteristic of the well known β/β and α/γ cycles have been prepared using experimental conditions which are known to favor each particular cycle. The β/β cycle materials were produced by cycling in an electrolyte solution of sufficiently high KOH concentration (4.2 M) to favor β-phase formation, and over a voltage range to avoid overcharge (-0.2 to 0.47 V, w.r.t. Hg/HgO/4.2 M KOH). The α/γ cycle materials were produced by cycling in electrolyte of lower KOH concentration (0.2 M) and over a voltage range that extended to a higher upper voltage (-0.2 to 0.56 V, w.r.t. Hg/HgO/0.2 M KOH). Cobalt was not added to these solutions because the objective was to define these four phases without the influence of an additive.

Other electrodes were prepared with various cobalt levels and commercial electrodes were tested which contained cobalt. Chemical γ-phases, β-phases and α-phases were prepared according to literature procedures. The detailed preparation conditions and the instrumentation used have been described in the publications and theses cited throughout this report.

RESULTS AND DISCUSSION: ELECTRODE STRUCTURE

The structural differences between the phases of active mass and precursor phases are seen by comparing the Raman spectra shown in Figure 1 (5,6). Figure 1 displays the Raman spectra of 3γ and 2α (6). The spectra of 3β and 2β are similar, but shifted in wavenumber to 550 and 468 cm^{-1}, and 532 and 468 cm^{-1}, respectively (7). It is clear that the four spectra of active mass (*i.e.* for the α/γ cycle and β/β cycle materials) are similar and that the four spectra differ from the β- and α-precursor spectra. The differences that are structurally significant are the different band **positions** and **relative intensity** differences. These data uniquely indicate structural differences. Most notably it is seen that the discharged active mass materials are not β-$Ni(OH)_2$. The different band positions for the two β-phases of the β/β cycle and the two α/γ cycle materials are indicative of more subtle, but significant, structural differences. (The important structural differences are layer stacking, crystal structure, nonstoichiometry, point defect structure, and oxidation state.)

Since the spectra for "precursor beta" and "active mass beta" differ, it has become necessary to modify the current nomenclature (*i.e.* Greek lettering) to further differentiate them. The same is true for precursor alpha and active mass alpha. We have proposed a simple method of differentiating the active mass materials by use of a "2" or "3" coefficient in front of α, β, or γ (5). The "two" or "three" represents the "nominal" oxidation state of these materials. This method has the benefit of **not** changing the traditionally used symbols so much that it is confusing, but does allow simple designation of an active mass material. When we use a Greek letter without a 2 or 3 coefficient, we then indicate a precursor phase which has **not been electrochemically cycled**. For example, this nomenclature allows distinction of the fact that the three beta-phases (β, 2β, and 3β) are NOT isostructural. This allows unique definition of each chemically or structurally different material. It should be noted that the Raman results show that a different preparation method generally generates a different structure.

To interpret the Raman spectra in terms of structure it is possible to first look to the literature at the well established structure of β-$Ni(OH)_2$ (12,13). It is the only material related to active mass for which the structure has been unambiguously defined. We have interpreted the Raman spectrum of this material in terms of the close packed layer stacking (ABAB) and the OH groups formed by protons bonding to the NiO_2 layers (7,8). Hydrogen atoms face one-another across the interlamellar space so that there is no hydrogen bonding between layers; however, these are not "free" OH groups. The Raman and IR spectra of β-$Ni(OH)_2$ are consistent with the selection rules predicted for the brucite crystal structure. It should be noted that β-$Ni(OH)_2$ is isostructural with brucite, $Mg(OH)_2$.

The vibrational spectra of brucite were analyzed by Mitra in 1962 (14). Jackovitz follows Mitra's analysis of this common structure in his paper on $Ni(OH)_2$ in 1982 (15). He uses Mitra's theoretical section

and structural figure, but he does not represent the vibrations of the NiO_2 layer lattice correctly. It is very important to note that the vibrations of a 3-dimensional lattice are not as simply understood as those for a small molecule. And, $Ni(OH)_2$ is <u>not</u> a small molecule with simple Ni-O stretches, simple O-Ni-O bends, O-H stretches, and Ni-O-H bends. Jackovitz incorrectly asserts that discharged active mass is β-$Ni(OH)_2$. He apparently assumed the conventional wisdom was correct about discharged active mass being β-phase, and simply ran the spectrum of $Ni(OH)_2$. He does not define the source of the $Ni(OH)_2$ in his paper, nor does he state that his $Ni(OH)_2$ spectrum was a scan of active mass (14). As we shall see shortly, his spectrum is clearly a scan of a disordered β-phase.

The Raman spectrum and Raman selection rules for β-$Ni(OH)_2$ indicate that there are two Ni-O lattice modes in the low wavenumber region. These can be assigned to vibrations of the NiO_2 layer lattice, primarily involving motion of the heavier atoms, nickel and oxygen. It is not possible to ascribe one to a stretch and one to a bend without further theoretical work. One Raman active O-H stretch is predicted and seen in the well known O-H stretching region of the spectrum. This motion involves the hydrogen moving against the NiO_2 layer. The IR spectrum is consistent with the predicted selection rules as well (16).

The Raman spectra of what we have come to term "disordered-β" phases (Barnard and co-workers first characterized these clearly and called them "deactivated phases (17)) have the same Raman bands as seen in recrystallized β-$Ni(OH)_2$ (highly ordered β-$Ni(OH)_2$), plus three additional bands (6). These Raman spectra demonstrate that these "deactivated" materials are disordered β-phases. We believe these bands are related to point defects in the lattice. These β-phases have broadened powder X-ray Diffraction (XRD) patterns, also indicative of this disorder. Barnard and co-worksers also reported the XRD patterns. In contrast with the distinct Raman spectra, the IR spectra of these disordered phases are quite similar to those of recrystallized β-$Ni(OH)_2$ and do not clearly show the unique structure of these materials (16).

The number and relative intensities of Raman bands are different for the β-type (close packed) spectra and active mass phases. The active mass Raman spectrum exhibits no O-H stretch bands, and the two lattice modes exhibit different wavenumber positions and a different intensity ratio. These positions and ratios differ among the four active mass spectra also.

To understand the structure represented by the active mass type spectrum we began to analyze the Raman spectrum of other related phases and found that the Raman spectrum of chemically prepared NiOOH (specifically γ-NiOOH) was the same, indicating these materials were isostructural (6). Since there are several structural interpretations for the γ-type materials, we re-analyzed the XRD patterns for these materials. We have been able to show that the XRD pattern for chemically prepared γ-NiOOH matches the predictions based on the $R\bar{3}m$ structure (with Z=1) better than those predicted for other more complex structures. This simple cell has ABBCCA type layer stacking and is

non-close packed. Glemser and Einerhand first suggested this structure type for NiOOH but later reported different structures, and more complex structures have been proposed by Bode *et al.* (18,19). The selection rules predicted for these other, more complex structures are inconsistent with the observed spectra.

Based on the above analysis, it can be seen that the non-close packed structure exhibits unique selection rules, which are clearly different than the close packed selection rules. Therefore, all four active mass phases exhibit a non-close packed structure (5-6). The two low wavenumber vibrations of the γ-type lattice are assigned to NiO_2 lattice modes, by analogy with the vibrations of β-$Ni(OH)_2$. The fact that there is no O-H stretching mode in these Raman spectra is consistent with the predicted Raman selection rules (5-6). The reason for this is not that there are no O-H vibrations in γ-NiOOH; rather, that these are Raman inactive because the hydrogen atoms are on centers of symmetry.

The Raman spectra of all four active mass phases are similar because they have the same basic structure, *i.e.* non-close packed (ABBCCA) NiO_2 layer stacking. All four exhibit different band positions, higher wavenumber upon charge and lower upon discharge. These reflect the increased Ni-O force constants accompanying a higher nickel oxidation state. This is a well known affect in coordination compounds (20). The relative intensities change consistently, in that the higher oxidation state materials exhibit a ratio close to one and the lower oxidation state materials exhibit a ratio closer to 0.5. The reason that the α/γ cycle band positions are higher than for the β/β cycle pair is that the former has higher oxidation states than the latter.

To understand the oxidation state differences and the empirical formula differences for these various phases, it is necessary to consider that these materials are nonstoichiometric and contain point defects. Nonstoichiometry is commonly exhibited in inorganic transition metal compounds, in particular those that exhibit "network" structures, not "molecular" structures. If two materials exhibit similar Raman and IR spectra and XRD patterns, then they must have similar crystal structures. If these two materials have different empirical formulae, then this variation must be accounted for in terms of nonstoichiometry within this crystal lattice. Nonstoichiometric materials generally contain point defects which make this all possible. Missing atoms (vacancies) and nickel atoms with oxidation states above 2 or 3 allow a reduction in nickel vs oxygen atoms ($Ni/O < 0.5$). The incorporation of hydrogen or potassium atoms on nickel sites or on interlamellar sites allows for the additions of potassium in the structure and the excess hydrogen contents ($H/O > 0.5$ for charged phases and $H/O > 1$ for discharged phases).

We proposed such a Nonstoichiometric, Point Defect Containing (NSPDC) structural model in 1986 (5). Analysis of empirical formulae for our own materials and those in the literature support this NSPDC model. The empirical formula for the 2α, 3γ, 2β, and 3β phases of Barnard *et al.* serve as a good example (17). These empirical formulae

can be re-cast into nonstoichiometric formulae (5-8). We define the ideal charged and discharged stoichiometries as NiOOH or $NiOOH_2$, respectively, within a common $R\bar{3}m$, Z=1 crystal lattice. Cations to the left of the two oxygen atoms are implied to be on the nickel sites (within NiO_2 layers); those to the right of the two oxygens, on interlamellar sites. The presence of higher valent nickel atoms (Ni^{3+} on Ni^{2+} sites of $NiOOH_2$ and Ni^{4+} on Ni^{3+} sites of NiOOH) is required to maintain charge balance and explain the higher average oxidations states observed. When cobalt is present, it is possible to define the nonstoichiometric formulae with cobalt atoms on nickel sites (Co_{Ni}) (8). It is interesting that the excess hydrogens and the potassiums can be fit on the nickel vacancy sites or on interlamellar sites to maintain these proposed site stoichiometries. We have, therefore, proposed that vacant nickel sites and interlamellar sites may hold protons, potassium atoms, and cobalt additive (5-8). Further research is needed to uniquely define which sites hold which atoms. The structurally simple picture which emerges is quite appealing.

A general equation for cycling is presented in the following equation (8):

$$[Ni_{Ni(1-x)}\ (nH)_{Ni(x)}]_{1.0}\ [OO\ H_H]_{2.0} + [x(n-1)+1]\ OH^- \xrightarrow{\text{charge}}$$

$$[Ni_{Ni(1-x)}\ (H)_{Ni(x)}]_{1.0}\ [OO\ H_H]_{1.0} + [x(n-1)+1]\ H_2O + [x(n-1)+1]\ e^-$$

Using this NSPDC model, the difference between the α/γ and β/β cycles is seen to be primarily a difference in nickel vacancy content, in addition to variation in oxidation state and Ni/O/H/K ratio (5). Empirically, it is interesting to note, that the two β/β phases have a common vacancy content of 0.11, and the two α/γ phases have a common vacancy content of 0.25. Empirical results indicate that the nickel vacancies, V_{Ni}, contain protons, $(nH)_{Ni}$, and that n is typically 2. For the α/γ cycle, where x=0.25, 1.25 electrons are transferred in this equation, which is equivalent to 1.66 electrons per nickel atom. The average oxidation states of the reactant and product would be 2+ and 3.66+, respectively. If there were no protons retained on the nickel vacancy of the charged product, 2 e^-/Ni would be transferred (product average oxidation state of 4+). If the materials retain potassium from the electrolyte, the average oxidation states would be reduced further, with a concomitant reduction in electron transfer. Clearly it is necessary to have knowledge of the proton and potassium contents to understand the structure and capacity of an electrode material.

Table I summarizes structurally significant observations drawn from the Raman results and the structural conclusions drawn from the nonstoichiometric model.

TABLE I

Summary of Major Structural Conclusions

Charged active mass has a γ-NiOOH type structure (non-close packed).
The four phases of active mass have a common non-close packed structure.
Discharged active mass is not isostructural with β-$Ni(OH)_2$, nor with α-phase materials; rather, it has a non-close packed layer structure similar to that of the charged material (but with a higher H-content).
α/γ and β/β cycles produce distinct spectra, allowing differentiation of these phases.
A disordered structural model, containing nickel vacancy point defects, is proposed for active mass.
Potassium incorporation may take place by substitution on vacant nickel sites, not only on interlamellar sites.
Cobalt incorporation appears to occur by substitution on nickel sites.

CAUSES OF ELECTRODE FAILURE

Using Raman spectroscopy, we have identified one cause for electrode failure. A second phase was observed in nickel electrodes which failed under high KOH conditions (10). The latter had failed via an undefined mechanism; the electrodes originated in a NASA supported study done by Hong Lim at Huhes Aircraft Company (9). The second phase content, as measured from the Raman spectra, was proportional to the KOH concentration. More recently we have identified the second phase found in the failed nickel electrodes by comparison of x-ray powder diffraction patterns (11). This comparison shows that the material formed is isostructural with a phase prepared previously by Malsbury and Greaves (21). It is interesting that they prepared this phase under high pressures. It is probably not coincidental that this phase forms in Ni/H_2 cells which do experience high pressures when charged. It should be noted that it was not observed in electrodes cycled in lower KOH electrolyte. The later failed by a "soft short" mechanism (9). These results suggest that lowering the KOH concentration and/or avoiding high pressure conditions (*e.g.* by using a metal hydride system) can improve cycle life.

EXAFS ANALYSES

EXAFS (Extended X-ray Absorption Fine Structure) spectra of nickel electrode materials were collected in 1986 at the National Synchrotron Light Source at Brookhaven National Laboratory for model compounds (α-, β-, and γ-phases, precursor phases and cycled materials). From data collected then, we have been able to show that:

a) physically realistic coordination numbers can be obtained (8,22),
b) the interlamellar thickness can be determined using the EXAFS and XRD results (23), and
c) point defects, specifically nickel vacancies, do show up as Ni-Ni coordination numbers less than 6 (24).

We used highly ordered, $Ni(OH)_2$ as a reference material. O'Grady and co-workers have reported unusually low coordination numbers and multiple shells (Ni-Ni and Ni-O) to interpret their data (25). Our interpretation, involving realistic coordination numbers, demonstrated that multiple shells were not necessary. What we do not understand, and which needs clarification, is why they have repeatedly observed multiple shells. Our EXAFS results provide an improved understanding of electrode structure and reactions; in particular, these EXAFS results support the NSPDC model proposed by us and discussed above (5-8).

THE FORMATION PROCESS, AGEING, AND β-PHASE FORMATION

When we consider that 2α, 2β, α, and β phases have different Raman spectra, and therefore different structures, the formation process can be understood. When a cathodic or chemical alpha phase (α) or beta phase (β or disordered-β) is cycled the structures are changed from that of the precursor to the non-close packed structure with extensive nickel vacancies. This process forms a black, active mass material from a generally green precursor. The green color is indicative of Ni(II), the black, of point defects including higher valent nickel. The formation process has been described in terms of the nonstoichiometry in more detail (7,8).

The ageing process forms disordered β-phase materials from α-phase materials, as first described by Barnard *et al.* (17). This process is clearly seen in the Raman spectra (6,7). Bernard describes these aged materials as "deactivated." We believe that it is the presence of aged β-phases that explains the origin of the β-type x-ray patterns which led to the naming of the β/β cycle. As discussed above, the Raman spectra of active mass (with and without cobalt) do not show a spectrum characteristic of a true β-phase material, only that of 2β or 2α. The fact that a small amount of an ordered material can give a stronger XRD pattern than a poorly ordered material explains why the β-phases are seen in the XRD and not the Raman (8). We have proposed that these observations suggest that the presence of β-phases may be detrimental.

THE STRUCTURE OF CATHODIC α-PHASE, COBALT ADDITION IN SITU RAMAN SPECTROSCOPY AND LAYER THICKNESS DETERMINATION

The structure of cathodic α-phase has traditionally been thought to be close packed and has been modeled after the β-phase structure in the literature (26). Raman data indicate that the cathodic α-phase is also non-closed packed (7). We have reinterpreted the XRD pattern in terms of this non-close packed structure and shown that the XRD pattern can be better explained with this model (27). That is, cathodic-α also exhibits ABBCCA stacking, as in active mass.

Cobalt addition has been studied as well (28,29). The influence of cobalt on the electrode structure and cobalt oxidation states was studied (see abstract in Appendix B for ref. 29).

In situ Raman spectra have been successfully collected (30,31). The report describing the "dynamic" collection procedure, run while the electrode is continuously cycling, is attached as Appendix A (32 and see abstract in Appendix B for ref. 30).

The layer thickness of the NiO_2 layer and the interlamellar spacing was uniquely measured for the first time, using a combination of XRD and EXAFS data (23). These measurements cannot be obtained from XRD alone. XRD only gives the total thickness, the sum of these two values. EXAFS analysis of the disordered β-phases was also reported (22 and Appendix B).

CONCLUSIONS

The following structural picture of nickel electrode active mass is emerging. The basic structural unit, an NiO_2 layer, is supported by our work; however, layer-layer stacking disorder and nonstoichiometry (*i.e.* nickel vacancy point defects) are believed to be extensive. The structures of charged and discharged active mass are very similar based on the fact that the vibrational spectra indicate that there is no change in selection rules. This suggests that the layer stacking does not change during cycling. The chemical bonding and bond distances do change during cycling as the nickel oxidation state changes and mobile cations (K^+,H^+) are incorporated. These vibrational spectral selection rules are consistent with the $R\bar{3}m$, Z=1 unit cell and ABBCCA structure(adjacent NiO_2 layers not close packed, the so-called γ-NiOOH structure). In contrast, spectra of β-type phases with close packed layer-layer stacking exhibit drastically different selection rules.

Raman spectra indicate that Barnard's deactivated material is structurally related to β-$Ni(OH)_2$, but is distinctly different. Therefore, we propose these phases be referred to as "disordered-β" phases. It is probably this material which accounts for the so-called β-type x-ray pattern in active mass; however, it is not isostructural with discharged active mass. Since it can be formed simply by KOH aging, observation of it may be misleading. Electrochemical measurements by Barnard *et al.* show that this is a less active material. Its presence in actual electrodes may, therefore, be detrimental.

The unique structure of active mass is induced during the formation process. The necessity of the formation process can be pictured with respect to this model. Formation appears to involve the transformation from close packed layers to ABBCCA stacking. It is concluded that the measure of quality for a precursor α-phase is determined by how close the structure of the starting material is to that of active mass. The cathodic deposition process is successful because it produces a material that is closer in structure to that desired for active mass with optimal properties. This "optimal structure" is discussed in terms of lattice disorder, including a significant nickel vacancy content.

The role of cobalt is also understood in this frame-work. We propose that cobalt incorporation favors this optimal structure. Spectral data suggest that cobalt addition stabilizes a structure that is γ-like, increasing capacity, but minimizing structural change upon cycling. It is likely that minimal change during cycling improves the mechanical integrity of the electrode.

Discharged active mass is not isostructural with α- or β-type materials. α- and β-type phases each provide different spectral signatures, which reflect structure variations.

The structures of the α/γ and β/β cycles then differ in the nickel vacancy content. Cycling can lead to loss of vacancies and transformation to the β/β cycle. Overcharging can introduce vacancies

and induce the α/γ cycle. A higher vacancy concentration provides greater capacity.

We therefore propose the key structural elements are the nickel vacancy concentration and the layer-layer stacking. The maximum concentration of vacancies is optimal, providing increased capacity, but apparently not the most stable. The non-close packing of layers provides an open structure for high proton mobility and requires no lattice movement (i.e. layer shear to closest packing) upon discharge.

It appears that additives such as Li or K enter the NiOOH lattice and, whether they reside on Ni sites or on interlamellar sites, stabilize the defective NiO_2 layer formation. Evidently Li or K incorporation increases the number of Ni^{3+} and/or the number of nickel vacancies, thereby stabilizing the point defect containing lattice. Because we have never seen an example where more than one mole of hydrogen and potassium is present, we propose that some K and Li can be incorporated on Ni sites.

A "new phase" has been identified using Raman spectroscopy which correlates with electrode failure. This material forms more easily with higher KOH concentration and apparently with the higher pressures present in a Ni/H_2 cell. This is the first definite identification and correlation of formation of a particular second phase with electrode failure.

In situ Raman experiments of charged active mass have been carried out successfully, and are not inconsistent with the *ex situ* data. Subtle structural changes are observable during cycling. This technique is expected to be a great aid in further understanding of the structure of discharged active mass, of the effect of cobalt addition, and of failure mechanisms.

Acknowledgements: This research has been carried out in collaboration with former graduate students Patricia L. Loyselle (Ph.D., M.S.), Xiaoyin Shan (Ph.D.) and Phillip J. Karjala (M.S.) in the Department of Chemistry. Their careful experimental work and efforts brought this study to fruition. An undergraduate, Steven J. Brownell, also contributed (with a Summer Senior Fellowship from the Dean of Engineering and the Dept. of Chemistry and Chemical Engineering). The many helpful discussions with Ralph Brodd, Dean C. Luehrs, Joseph Singer, Hong Lim, Sidney Gross, Robert Pipal, James C. Phillips, Joseph Stockel, Albert Zimmerman, James McBreen, and Hari Vaidyanathan are greatly appreciated.

Both the fiscal and technical support from NASA, Lewis Research Center are gratefully acknowledged. The author especially appreciates the collaboration with Margaret Reid. The author is also grateful to Michigan Technological University, the New York State College of Ceramics at Alfred University, and the National Synchrotron Light Source (NSLS), at Brookhaven National Laboratory, for the opportunity to conduct EXAFS (Extended X-ray Absorption Fine Structure) experiments (supported by the DOE) at the NSLS during his sabbatical leave in 1986.

REFERENCES

1. Bahne C. Cornilsen, "Raman Structural Studies of the Nickel Electrode," Summary Report, NASA Lewis Research Center, Cleveland, OH, Grant No. NAG 3-519 (Power Systems Division), Feb. 20, 1984 - March 20, 1985.

2. P. L. Loyselle, D. C. Luehrs, and B. C. Cornilsen, "Nickel Electrode Structures," 168th Electrochemical Society Meeting, Abstract 26, Las Vegas, NV, October 16, 1985.

3. Bahne C. Cornilsen, "Raman Structural Study of Nickel Electrodes", Seminar, General Motors Research Labs, Warren, MI, January 9, 1986.

4. B. C. Cornilsen and P. J. Karjala, "Comparative Study of Nickel Oxide and Oxyhydroxide Structures," 88th Annual American Ceramic Society Meeting (Proceedings of the Electronics Division), Chicago, IL, April 30, 1986.

5. P. L. Loyselle, P. J. Karjala, and B. C. Cornilsen, "A Point Defect Model for Nickel Electrode Structure," in Electrochemical and Thermal Modeling of Battery, Fuel Cell, and Photoenergy Conversion Systems, Proceedings Vol. 86-12 (J.R. Selman and H.C. Maru, Eds.), The Electrochemical Society, Pennington, NJ, 1986, pp. 114-21.

6. B. C. Cornilsen, P. J. Karjala, and P. L. Loyselle, "Structural Models for Nickel Electrode Active Mass," J. Power Sources, 22 351-7 (1988).

7. B. C. Cornilsen, X. Shan, and P. L. Loyselle, "Structural Comparison of Nickel Electrodes and Precursor Phases," J. Power Sources, 29 453-66 (1990).

8. B. C. Cornilsen, X. Shan, and P. L. Loyselle, "The Structure and Reactions of the Nickel Electrode," in Nickel Hydroxide Electrodes, Proceedings Vol. 90-4 (A. H. Zimmerman and D. A. Corrigan, Eds.), The Electrochemical Society, Pennington, NJ, 1990, pp. 82-96.

9. H. S. Lim, Final Report, "Nickel Electrode Research," Contract 89-F765100, Hughes Aircraft Company, Torrance, CA, June, 1992.

10. P. L. Loyselle, X. Shan, and B. C. Cornilsen, "Raman Spectral Observation of a "New Phase" Observed in Nickel Electrodes Cycled to Failure," J. Power Sources, 36 279-284 (1991).

11. B. C. Cornilsen, P. L. Loyselle, and M. A. Reid, "Identification of a second phase found in failed nickel electrodes," to be submitted.

12. P. M. De Wolff, Joint Committee on Powder Diffraction Standards, Card No. 14-117.

13. A. Szytula, A. Murasik and M. Balanda, Phys. Status Solidi B, 43 125-128 (1971).

14. S. S. Mitra, Solid State Physicis, Vol. 13 (F. Seitz and D. Turnbull, Eds.), 1962, pp. 1-80.

15. J. F. Jackovitz, "The Vibrational Spctra of Nickel Hydroxide and Higher Nickel Oxide," in The Nickel Electrode, Proceedings Vol. (R. G. Gunther and S. Gross, Eds., The Electrochemical Society, Pennington, NJ, 1982, pp. 48-68.

16. Patricia L. Loyselle, "Raman Spectroscopic Study of Nickel Electrode Materials," M.S. Thesis, Michigan Technological University, 1985.

17. R. Barnard, C. F. Randell, and F. L. Tye, Power Sources 8, (J. Thompson, editor), Academic Press, London, 1981, p. 401.

18. O. Glemser and J. Einerhand, Z. anorg. allg. Chemie, 261, 43-51 (1950).

19. H. Bartl, H. Bode, G. Sterr and J. Witte, Electrochemica Acta, 16, 615-621 (1971).

20. K. Nakamoto, Infrared and Raman Spectra of Inorganic and Coordination Compounds, 4th Edition, John Wiley and Sons, New York, 1986.

21. A. M. Malsbury and C. Greaves, J. Solid State Chem. 71 418-425 (1987).

22. P. L. Loyselle, B. C. Cornilsen, R. A. Condrate, and J. C. Phillips, "X-ray Absorption Study of Beta-Nickel Hydroxides," 174th Electrochemical Society Meeting, Chicago, IL, October 14, 1988, Extended Abstracts of Battery Division, Abstract No. 77, p. 117.

23. P. L. Loyselle, B. C. Cornilsen, R. A. Condrate, and J. C. Phillips, "Empirical Measurement of NiO_2 Layer Thickness and Interlamellar Spacing for Charged and Discharged Nickel Electrode Active Mass," The Electrochemical Society Fall Meeting, Seattle, WA, Oct. 14-19, 1990, Extended Abstracts of Battery Division, Abstract No. 71, p. 115.

24. Patricia L. Loyselle, "EXAFS Structural Study of Nickel Electrode Materials," Ph.D. Thesis, Michigan Technological University, 1989.

25. W. E. O'Grady, Synchrotron Radiation News, 6, 25-29 (1993) and references therein.

26. H. Bode, K. Dehmelt, and J. Witte, Electrochim. Acta, 11, 1079 (1966).

27. Philip J. Karjala, "Structural Studies of Nickel Electrode Model Compounds," M.S. Thesis, Michigan Technological University, 1987.

28. Xiaoyin Shan, "Structural Study of the Influence of Cobalt on the Nickel Electrode," Ph.D. Thesis, Michigan Technological University, 1990.

29. X. Shan, P. L. Loyselle, and B. C. Cornilsen, "Structural Influence of Cobalt Addition to the Nickel Electrode," 174th Electrochemical Society Meeting, Chicago, IL, October 14, 1988, Extended Abstracts of Battery Division, Abstract No. 79, p. 120.

30. B. C. Cornilsen and P. L. Loyselle, "*In situ* Raman Spectra of the Nickel Electrode," 174th Electrochemical Society Meeting, Chicago, IL, October 14, 1988, Extended Abstracts of Battery Division, Abstract No. 78, p. 118.

31. P. L. Loyselle, X. Shan, and B. C. Cornilsen, "Structural Investigations of the Nickel Electrode Using *In situ* Raman Spectroscopy," The Electrochemical Society Fall Meeting, Hollywood, FL, Oct. 15-20, 1989, Extended Abstracts of Battery Division, Abstract No. 105, p. 159.

32. Bahne C. Cornilsen, "Raman Structural Studies of the Nickel Electrode," Summary Report, NASA Lewis Research Center, Cleveland, OH, Grant No. NAG 3-519 (Power Systems Division), Oct. 17, 1987 - Sept. 15, 1988.

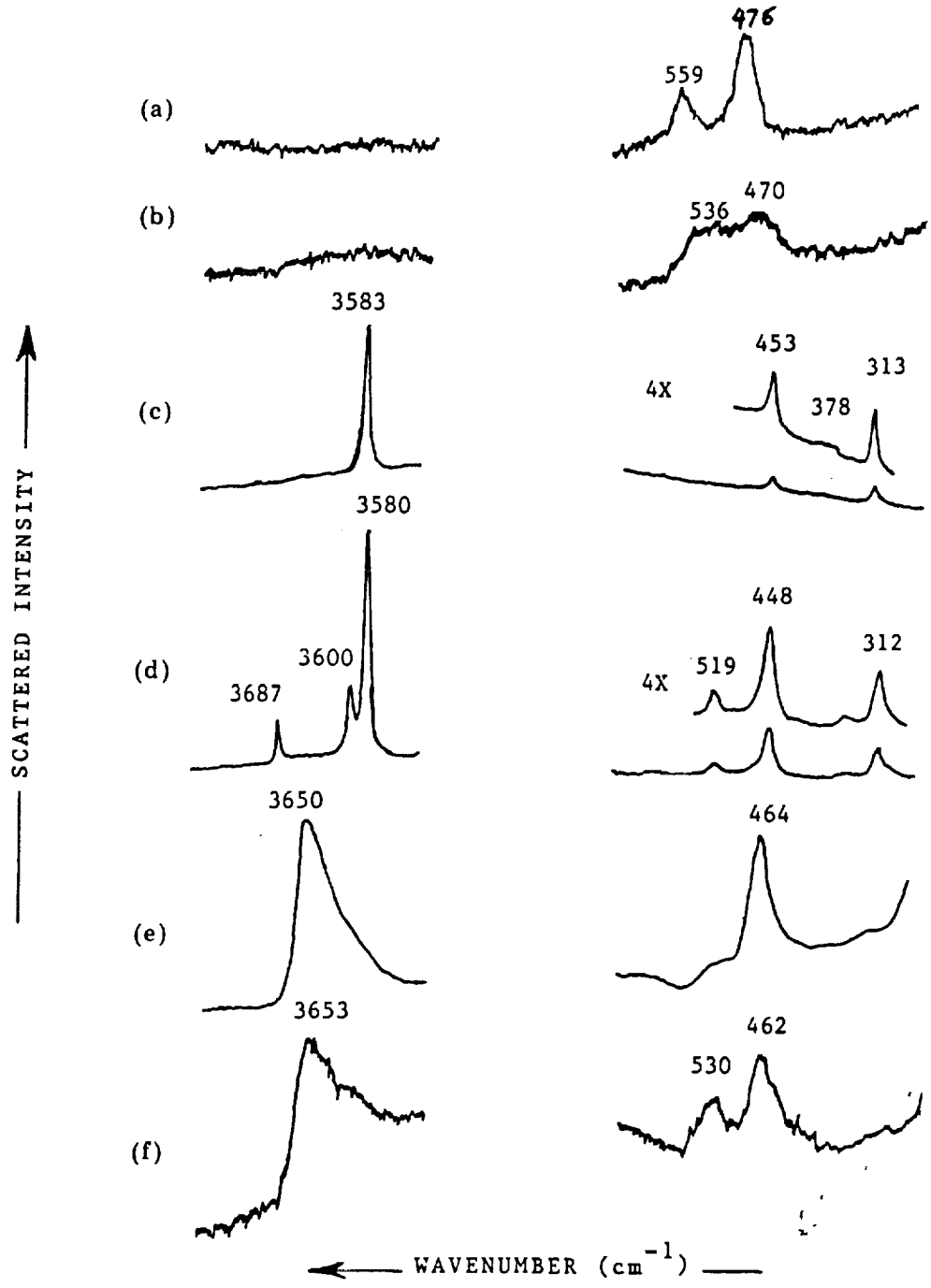

Fig. 1. Raman spectra of nickel electrode active mass and model compounds. (a) Charged γ active mass; (b) discharged α active mass; (c) recrystallized β-$Ni(OH)_2$; (d) first precipitate β-phase; (e) chemical-α; (f) cathodic-α.

Appendix A

RAMAN STRUCTURAL STUDIES OF THE NICKEL ELECTRODE

(Power Systems Division)
(Grant NAG 3-519)

SEMI-ANNUAL REPORT for
October 17, 1987 - Sept. 15, 1988

Submitted
January 20, 1989

Bahne C. Cornilsen

Michigan Technological University
Department of Chemistry and Chemical Engineering
Houghton, MI 49931

Sponsor:
University Grants Office
National Aeronautics and Space Administration
Lewis Research Center
21000 Brookpark Avenue
Cleveland, OH 44135

Introduction

During this period of research we have completed the development of the apparatus to allow simultaneous computer control of the Raman instrument and the potentiostat. This allows "dynamic" collection of *in situ* Raman spectra while the Cyclic Voltammetry (CV) scans are in progress, making it possible to characterize structural changes during charge and discharge. By varying empirical parameters (*e.g.* cobalt content or KOH concentration), we can now chart structural differences induced by each change in variable. This technique, therefore, makes it possible to both define and control optimal electrode structures, and thereby, to optimize the electrochemical behavior. Constant current charge and discharge is also possible.

This Dynamic *In Situ* Electrochemical Raman Technique (DISERT) has, therefore, been demonstrated for the first time. We have demonstrated that the software and hardware operate as designed and that the system can produce results meeting expectations.

Experimental results are also reported from our preliminary study of structural change at high Depth of Discharge (DOD). The chosen electrode exhibits a secondary plateau below *ca.* 94% DOD. Constant current charge/discharge experiments indicate the presence of a previously unobserved phase at high DOD. The introduction of this phase may explain why nickel electrodes work well up to 80% DOD, but behave differently at higher DOD. We do not know, as yet, whether such a phase might be associated with a secondary plateau when the plateau occurs at much lower DOD.

Other recent work on static *in situ* Raman spectra, cobalt doping, and EXAFS of β-$Ni(OH)_2$ is summarized in three extended abstracts of papers delivered at the October, 1988, Electrochemical Society Meeting in Chicago (see Appendix).

Additional electrochemical and structural results were obtained this summer from studies by three undergraduate students, Angela Garcia (from St. Catherines College), Susan Kellaher (Alfred University), and Lydia Tiedje (MTU). They are three of eight students supported by an NSF REU (Research Experience for Undergraduates) grant to the Department of Chemistry and Chemical Engineering (1). Dr. Dean C. Luehrs and I supervised them on studies of a) cobalt hydroxide and oxyhydroxide model compounds, b) average oxidation states and nonstoichiometry of chemically oxidized cathodic deposits, and c) structural changes in the discharge products of an MnO_2-Li cell.

Instrumentation and the Dynamic *In Situ* Electrochemical Raman Technique

The experimental results reported herein have been made possible by recent instrumentation improvements over the past year. These include improved spectral subtraction, computer control of the Raman for the DISERT, and computer control of the potentiostat. In July of 1987 a new stepping motor (in the monochromator) and the Spectra Link data acquisition and control system for the Raman instrument were installed. Normally the Spectra Link system is controlled by the ISA (Instruments S A, Inc.) "Prism" software on the IBM XT computer. We had hoped to use this software for the dynamic *in situ* experiments; unfortunately, neither of the first two software versions have allowed intensity/time plots at sequential wavelength positions. Therefore, it has been necessary to bypass the Prism software and control the Spectra Link directly with a program written by us.

Computer control of the potentiostat is necessary for the dynamic experiments. This has been accomplished using a Keithley System 570 data acquisition and control system together with an IBM Personal Computer (PC or XT). This control is needed on a practical basis, because of the length of time required for a dynamic *in situ* experiment (48 to 96 hrs.), but also to improve reproducibility of voltammogram scans. Current, time, wavenumber position, and intensity values are all logged on the computer. A corresponding amount of data using static *in situ* Raman would require three to five times as much time. Furthermore, the results would be perturbed by stopping the cyclic voltammograms for spectral collection.

The software for control of the Raman and the potentiostat (for DISERT) was completed and tested in May and June, respectively (1988). More recently we finished writing programs to control the galvanostat during constant current cycling. These allow a) Raman studies of *ex situ* electrodes which have been cycled many more times (more than one to fifteen times) under highly reproducible conditions, and b) constant current *in situ* studies. Therefore, we can now study structural changes after extensive cycling. Constant current results can be compared with CV data.

The Dynamic *In Situ* Electrochemical Raman Technique (DISERT) allows one to monitor structural changes which occur during cycling, while they are taking place, and eliminates outside interferences. Most other techniques used in the elucidation of structure require that the cyclic voltammogram be interrupted and/or the electrode be removed from the electrolyte. Such interruptions can change the electrode structure (aging, self-discharge). This perturbation can, in turn, change the reaction following the interruption. DISERT avoids these problems by not introducing any unnecessary

perturbations into the electrochemical system. The spectral data are collected while a series of uninterrupted voltammograms are cycled reproducibly.

The DISERT measures the Raman intensity at a constant wavenumber during an entire CV scan. Then the wavenumber is changed and another CV is run. Enough wavenumber positions are used to adequately define the spectrum of the electrode. The number of wavenumber positions required is determined by the band positions and spectral shifts expected from earlier *ex situ* and static *in situ* experiments. These intensity/voltage data (at a series of wavenumber positions) are reconstructed into intensity/wavenumber plots (spectra) as a function of potential, Figures 1 and 2, respectively. See the first abstract in the Appendix also. Such "dynamic" spectra have been previously conducted using IR spectroscopy, but not Raman spectroscopy.

Constant Current Experiments

The intention of this preliminary experiment was to characterize the structural changes, if any, which occur in the electrode active mass near the secondary discharge plateau, at high DOD, for a plaque electrode.

Initial experiments involving the constant current charge and discharge of an electrode were done using a formed, Eagle Picher sintered plaque electrode (as-received). It was reduced in size to 1.1 cm x 2.5 cm to reduce the capacity. This electrode was used previously to prove the feasibility of the dynamic *in situ* experiment, and had undergone *ca.* 30 prior cycles. The measured capacity was 40.0 mA·hr, based on a C/10 rate.

During the constant current experiment, the electrode was cycled in 7.0 M KOH and the electrode potential was measured with respect to a Hg/HgO/7.0 M KOH reference electrode. The electrode was charged and discharged using a C/10 (4 mA) rate. Spectra of the electrode active mass were collected at the following five levels of charge or discharge:

Sample No. NI57,	130.0%	Charge
Sample No. NI56,	84.2%	Discharge
Sample No. NI61,	91.0%	Discharge
Sample No. NI60,	92.3%	Discharge
Sample No. NI59,	100.0%	Discharge

Throughout most of the discharge the change in electrode potential was small. However, after the electrode had been discharged *ca.* 85%, the potential began to change more rapidly, with a steep drop starting below *ca.* 94% and ending in a small plateau (the secondary plateau).

For the five spectra collected during this experiment, the most striking change was observed between the totally charged and discharged electrodes. Not only do the peak frequencies and intensities change between the two but a shoulder was present on the high frequency peak in the discharged spectrum. Spectra similar to this totally discharged electrode have been observed previously during static experiments under controlled potential. In the latter this spectrum began to appear only when the electrode was cycled to potentials below 100 mV.

The first four spectra, totally charged through 92.3% discharge, are strikingly similar. Each spectrum contains two bands in the lattice mode region (200 - 800 cm^{-1}) and none in the OH stretch region (3500 - 3800 cm^{-1}). Upon closer examination subtle differences are evident. The Raman band positions, while identical for the charged and 84.2% discharged spectra, are lower in the spectra of the 91.0% and 92.3% discharged electrodes (see Table I). The intensity and area ratios for the spectra also differ as a function of discharge state.

Table I. Spectral Parameters* for Plaque Electrode during Constant Current Discharge

Spectrum No.	Discharge State	Wavenumber (cm^{-1})	$\frac{I_{5--}}{I_{4--}}$*	$\frac{I_{536}}{I_{468}}$	$\frac{A_{5--}}{A_{4--}}$
NI57	130.% Charge	471 547	0.378	0.148	0.315
NI56	84.2% Discharge	471 547	0.392	0.212	0.370
NI61	91.0% Discharge	465 545	0.428	0.313	0.449
NI60	92.3% Discharge	466 543	0.344	0.318	0.349
NI59	100.% Discharge	468 537 587 sh	0.362	0.402	0.595

* The 5-- and 4-- designations refer to the 547-537 and 471-466 cm^{-1} bands, respectively.

Spectra of the totally charged and 84.2% discharged electrode appear to be nearly identical. Not only are the Raman peak frequencies the same, but also the intensity ratios

(I_{5--}/I_{4--}) (within experimental error). This consistency might imply that the active mass phases in the two electrodes are identical. While it is possible that the charged electrode underwent self-discharge, it is unlikely that the electrode would discharge completely. This view is supported by the observation that the area ratios for the two spectra are not the same. The change in the area ratios, with the intensity ratios remaining constant, implies that one of the Raman bands is broadening relative to the other. Such broadening could be caused by structural change as bands shift upon discharge or as new bands are introduced.

In general, intensity and area ratios differ for the electrode spectra at the various states of discharge. However, these ratios do not seem to change systematically with state of discharge (see I_{5--}/I_{4--} and A_{5--}/A_{4--} in Table I). Eventually, when the electrode is fully discharged, the Raman peak frequencies decrease to 468 and 537 cm^{-1}. In order to better understand the changes occurring with discharge, the intensities at two constant frequencies (468 and 537 cm^{-1}) were measured and ratioed. (That is, we are not measuring the ratios at the peak maxima for every sample.) This intensity ratio increases monotonically and consistently as the electrode is discharged, with the largest change occurring after the electrode reached 84.2% DOD. The increase in the intensity ratio, I_{537}/I_{468}, implies that as the electrode is discharged a new band grows in at 537 cm^{-1}. This new band could be caused by either a shift in the wavenumber position of one of the other bands (*i.e.* uncovered) or by the presence of a new phase.

To test for the existence of a new phase in discharged active mass, spectral subtractions were done on the spectra at each level of discharge. The totally charged spectrum was subtracted from each of the other electrode spectra. After subtraction, a residual spectrum (with three bands) remained for the 91% and 92.3% discharged electrodes. It was not found in the spectrum of the 84.2% discharged electrode. If the two residual spectra (for the 91% and 92.3% discharged samples) are normalized and subtracted from each other, a flat baseline remains. This demonstrates that the two residual spectra are identical. This residual spectrum appears to indicate the presence of an additional or new phase which is observed only above 90% DOD. If the peak areas are summed for the new phase and the original spectrum and then divided, the relative concentration of the new phase can be determined for each charge state. The concentration of new phase increases as the electrode is discharged.

The spectrum of this new phase, as obtained by subtraction, exhibits three bands at 582, 533, and 456 cm^{-1}. The former is clearly that seen as a shoulder at 587 cm^{-1} in the fully discharged spectrum. The O-H stretch regions for

the above mentioned samples do not show any Raman bands. Also the band positions and intensities in the lattice-mode region are different than those for a β-type material. Therefore, this new phase or phases is not a β-$Ni(OH)_2$ nor a disordered β-$Ni(OH)_2$. This phase and the spectrum for it also differ from those for the "new phase" which we previously observed in failed electrodes (2).

The origin of this phase will be probed in further experimental work. It could be a phase formed as a discharge product (or by-product). Alternatively, it may be a second phase which is present in the charged state as well, but one which does not exhibit a spectrum that is distinguishable from that of charged active mass. The latter seems less likely, but can not yet be eliminated. The new phase has been observed above 84% DOD and may only occur above 84%. Therefore, this circumstantial evidence implies that the presence of this new phase is detrimental to long electrode life.

The origins of this behavior may be structural. Theoretical selection rules predict three lattice modes for a close packed NiO_2 layer stacking. Therefore, it is possible that this new phase is close packed. If so, it is not surprising that the formation of this type layer stacking would be detrimental to electrode life. The transformation from the non-close packed active mass to the close packed form would involve a considerable change in volume. Any structural phase transformation is expected to be detrimental because concomitant density changes will lead to macroscopic deformation and shape changes. Structural integrity of the active mass in the plaque would suffer. Furthermore, it is likely that this close packed structure would resist transformation back to a non-close packed active mass during charge. We believe the application of the DISER Technique will be able to elucidate the critical detail of these constant current discharge results and secondary plateau studies.

References

1. D. Chesney, B. Cornilsen, D. Luehrs, and D. Hubbard, "Establishment of an REU Site for Fundamental and Applied Electrochemical Studies," National Science Foundation, Research Experience for Undergraduates, Summer, 1988.

2. B. C. Cornilsen, Semi-Annual Report to NASA-Lewis Research Center, for March 1, 1987 - October 16, 1987.

Figure 1

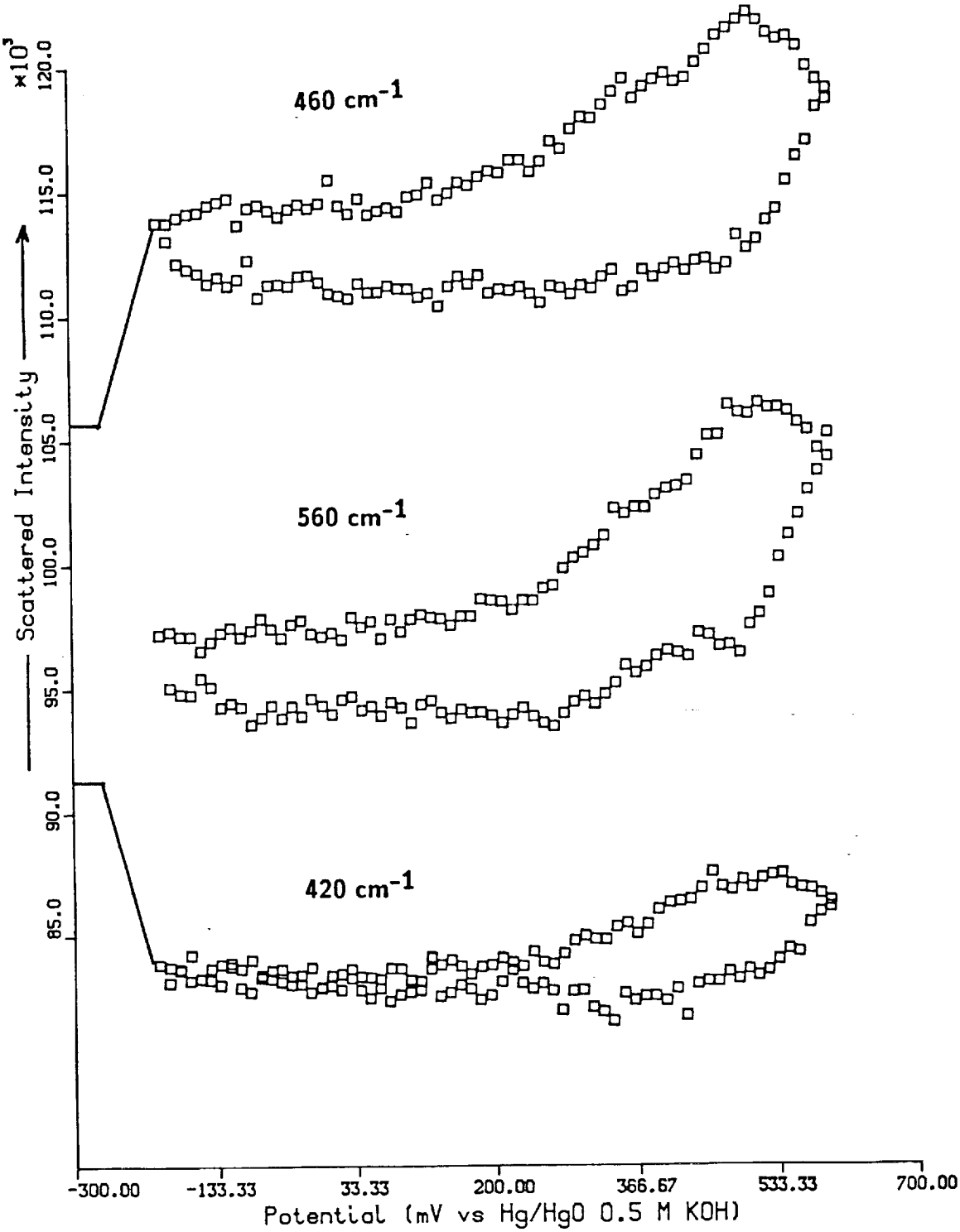
460 cm-1
560 cm-1
420 cm-1
Scattered Intensity
×10³
120.0
115.0
110.0
105.0
100.0
95.0
90.0
85.0
-300.00
-133.33
33.33
200.00
366.67
533.33
700.00
Potential (mV vs Hg/HgO 0.5 M KOH)

Figure 2

RAMAN SPECTRAL DEPENDENCE UPON VOLTAGE DISCHARGE

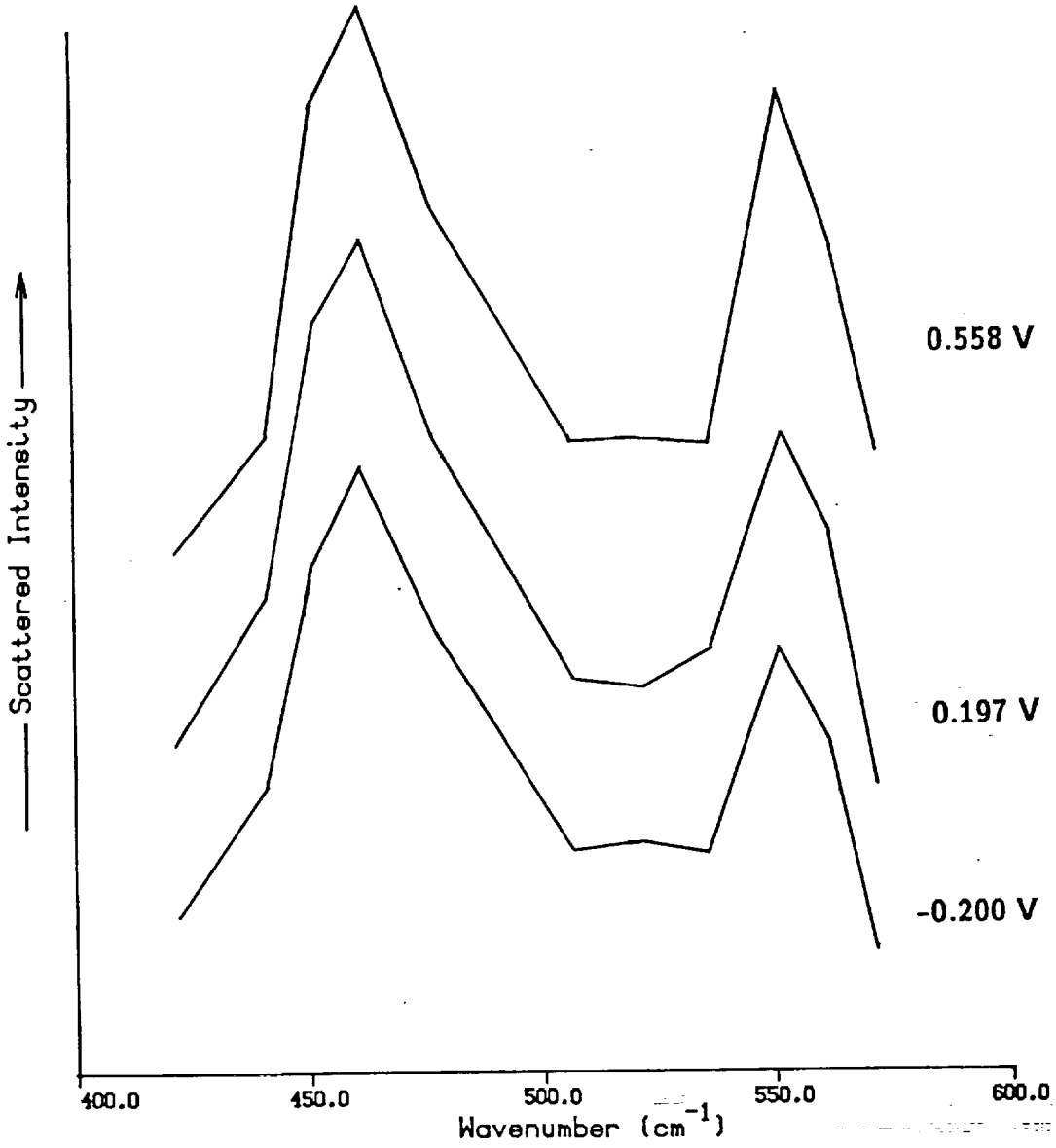

Appendix B

Extended Abstracts of three papers given at the October, 1988, Electrochemical Society Meeting in Chicago, Ill.:

"*In Situ* Raman Spectra of the Nickel Electrode,"
Bahne C. Cornilsen and Patricia Loyselle (ref. 30)

"Structural Influence of Cobalt Addition to the Nickel Electrode," (ref. 29)
Xiaoyin Shan, Patricia Loyselle and Bahne C. Cornilsen

"X-ray Absorption Study of β-Nickel Hydroxides,"
Patricia Loyselle, Bahne C. Cornilsen, Robert A. Condrate, and James C. Phillips (ref. 22)

In Situ Raman Spectra of the Nickel Electrode

Bahne C. Cornilsen and Patricia L. Loyselle
Dept. of Chemistry and Chemical Engineering
Michigan Technological University
Houghton, MI 49931

Extreme care must be taken to define the starting material used in any electrochemical study of a nickel electrode because of the diversity of structures which can be produced within the normal ranges of the experimental variables. The electrochemistry is strongly influenced by the precursor structure. Diverse structural phases can be differentiated using laser Raman spectroscopy, phases which cannot be distinguished using other methods (1,2). Furthermore, unique solid state structural information can be extracted from the spectra.

In situ Raman spectra of plaque electrodes have been studied, under controlled potential. Thin film electrodes are compared with formed and cycled plaque electrodes. The structural influence of cobalt addition can be observed. These structures will be contrasted with the cathodic alpha-phase precursor structure. We have also shown that *in situ* spectra can be collected during cyclic voltammetry scans (Fig. 1).

The *in situ* results confirm conclusions drawn from *ex situ* Raman spectra (1,2). Spectra in Fig. 2 demonstrate the structural similarity. 1) The spectra of active mass differ from those observed for the traditional model compounds. 2) Discharged active mass is not isostructural with α-$Ni(OH)_2$ nor with β-$Ni(OH)_2$. 3) The structure of discharged active mass is more closely related to that of charged active mass. 4) Charged active mass has a nonstoichiometric, non-close packed layered structure in the NiOOH space group. These results demonstrate the potential of *in situ* Raman spectroscopy for the study of electrode structures and their influence on the electrochemistry.

This work has been supported by NASA-Lewis Research Center.

References

1. P. L. Loyselle, P. J. Karjala, and B. C. Cornilsen, Proc. Symp. on Electrochemical and Thermal Modeling of Battery, Fuel Cell, and Photoenergy Conversion Systems, edited by J. R. Selman and H. C. Maru, Electrochemical Society, Pennington, NJ, 1986, p. 114.

2. B. C. Cornilsen, P. J. Karjala, and P. L. Loyselle, J. Power Sources, 22 (1988) 351.

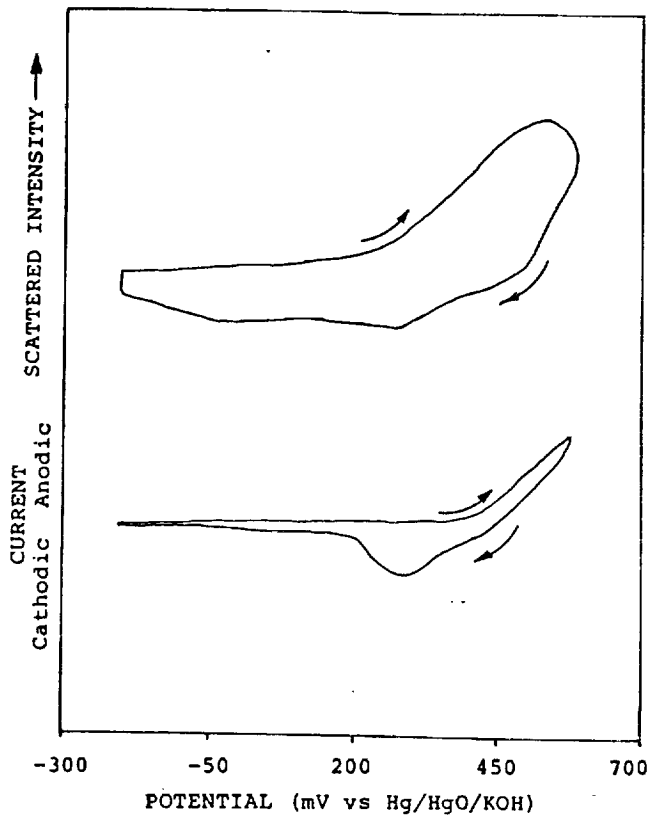

Figure 1. Simultaneous *In situ* Raman intensity at 550 cm^{-1} (a) and cyclic voltammogram (b).

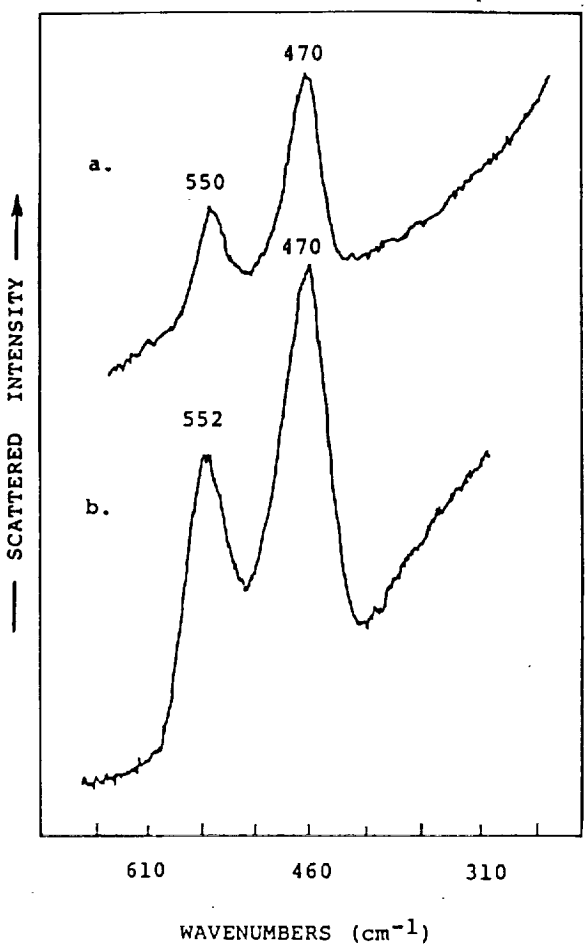

Figure 2. Comparison of *ex situ* (a) and *in situ* (b) Raman spectra of a plaque electrode. *Ex situ* removed after equilibrium at +0.48 V (vs Hg/HgO/KOH). *In situ* electrode held at +0.475 V.

Structural Influence of Cobalt Addition to the Nickel Electrode

Xiaoyin Shan, Patricia L. Loyselle, and Bahne C. Cornilsen

Department of Chemistry and Chemical Engineering

Michigan Technological University
Houghton, MI 49931

Cobalt is added to nickel electrodes to improve electrochemical properties such as capacity, conductivity, and cycle life (1,2). The objective of the research discussed today is to develop an understanding of how the cobalt improves the electrode, from a structural point of view. To do this we have studied the structures of electrode precursors (cathodic alpha phases) before and after cycling in KOH. The influence of cobalt has been measured by varying the cobalt concentration and comparing doped to undoped materials. Structure changes have been monitored using cyclic voltammetry and vibrational spectra, Raman and FT-IR spectroscopy.

Without cobalt, as deposited materials and cycled materials have different structures (3,4). However, the addition of cobalt enhances this difference. The structure of the cobalt containing cathodic deposit is drastically different from that deposited without cobalt (see Fig.1). Variation of the cobalt concentration also influences the structure of the precursor. After charging and cycling, spectra indicate that the active mass incorporates the cobalt by substitution on nickel sites in the nonstoichiometric NiOOH-type oxyhydroxide. We propose that the cobalt stabilizes a unique and optimum, nonstoichiometric NiOOH structure. Our earlier spectroscopic results showed that active mass contains significant nonstoichiometry which enhances proton and electronic conductivities in the solid state (3,4).

These results suggest that cobalt controls the structure of the active mass by way of controlling the precursor structure. Design of an optimum precursor structure (including the optimum nonstoichiometry) will allow control and improvement of electrochemical properties.

References

1. A. H. Zimmerman and P. K. Effa, J. Electrochem. Soc., 131 (1984) 709.

2. David H. Fritts, J.T. Maloy, J. Electrochem. Soc., 125 (1978) 1026.

3. P. L. Loyselle, P. J. Karjala, and B. C. Cornilsen, Proc. Symp. on Electrochemical and Thermal Modeling of Battery, Fuel Cell, and Photoenergy Conversion Systems, edited by J. R. Selman and H. C. Maru, Electrochemical Society, Pennington, NJ, 1986, p. 114.

4. B. C. Cornilsen, P. J. Karjala, and P. L. Loyselle, J. Power Sources, 22 (1988) 351.

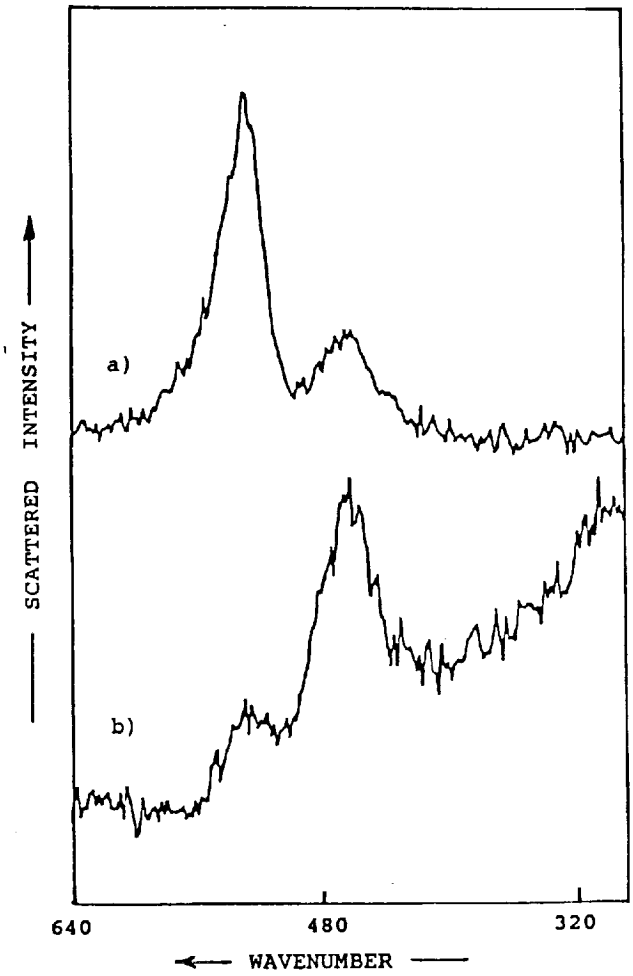

Figure 1. Raman spectrum of cathodic α-$Ni(OH)_2$ in the lattice mode region; a) containing 10 % cobalt, and b) without cobalt.

X-ray Absorption Study of β-Nickel Hydroxides

Patricia L. Loyselle and Bahne C. Cornilsen
Dept. of Chemistry and Chemical Engineering
Michigan Technological University
Houghton, MI 49931

Robert A. Condrate
New York State College of Ceramics
Alfred University
Alfred, NY 14802

James C. Phillips
National Synchrotron Light Source
Brookhaven National Laboratory
Upton, NY 11973

The EXAFS spectrum for ordered β-$Ni(OH)_2$ is interpreted in terms of the known crystal structure for this material and compared with the EXAFS spectra of disordered β-type hydroxides. The experimental pattern has been fitted using crystallographic bond distances and coordination numbers for the first four shells (Figure 1). These parameters are summarized in Table I. Additional shells, at higher radii, contribute to the spectrum but do not correspond to crystallographic distances. These may involve multiple scattering events.

A comparison of absorption edges (E_0) for the ordered material with those for disordered β-$Ni(OH)_2$ materials shows a dramatic shift to higher energy for the latter. Shifts in E_0 are known to be dependent upon oxidation state, coordination number and type of bonding (1). These materials contain no active oxygen but do exhibit unique Raman spectra which indicate coordination number changes (2).

These results indicate that care must be taken when interpreting nickel edge shifts for nickel electrode materials in terms of oxidation state changes alone. A shift in E_0 may result from a change in coordination number as well as oxidation state. Coordination number changes are significant in beta-nickel hydroxides and are expected to be significant in active mass as well.

This work is part of a study of nickel electrode "model compounds." The EXAFS spectra were collected on the SUNY beamline, X21, at the National Synchrotron Light Source at Brookhaven National Laboratory. The Dept. of Energy supported part of this research.

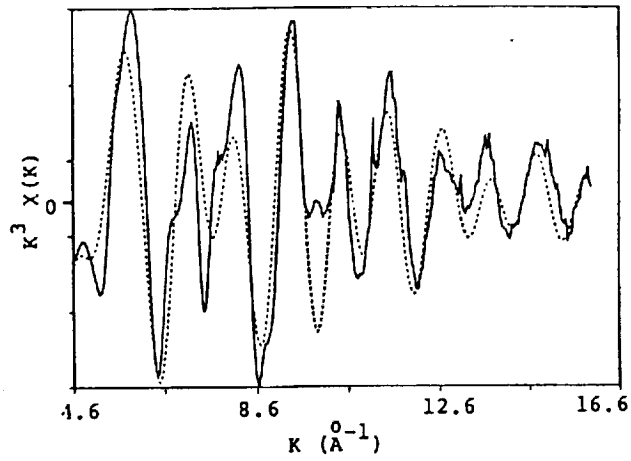

Figure 1. Calculated (dotted line) and experimental (solid line) EXAFS spectra of recrystallized β-$Ni(OH)_2$.

Table I

Shell	Coordination Number	Radius	Debye-Waller Factor
Ni-O	6	2.116	0.067
Ni-Ni	6	3.126	0.069
Ni-O	6	3.775	0.072
Ni-O	6	3.938	0.077

References

1. J. C. J. Bart, Advances in Catalysis, Vol. 34, edited by D. D. Eley, H. Pines, and Paul B. Weisz, Academic Press, Inc., New York, 1986, p.203

2. B. C. Cornilsen, P. J. Karjala, and P. L. Loyselle, J. Power Sources, 22 (1988) 351.